Journal of Pharmaceutical, Chemical and Biological Sciences
ISSN: 2348-7658
CODEN: JPCBBG
June - August 2018; 6(2):85-96
Online available at https://www.jpcbs.info

Research Article

Nano CuO Immobilized Zeolite Photocatalyst from Coal Fly Ash for Visible Light Photodegradation of Methylene Blue without H_2O_2

N. L. Subbulekshmi, E. Subramanian*
Department of Chemistry, Manonmaniam Sundaranar University, Tirunelveli 627 012, Tamil Nadu, India

***CORRESPONDING AUTHOR**
E. Subramanian, Department of Chemistry, Manonmaniam Sundaranar University, Tirunelveli 627 012, Tamil Nadu, India.
E-mail: esubram@yahoo.com

ARTICLE INFORMATION
Received January 29, 2018
Revised March 02, 2018
Accepted April 20, 2018
Published August 05, 2018

ABSTRACT
A new visible light active zeolite NaX photocatalyst was developed from coal fly ash (FA). First zeolite NaX (Zeo-NaX) was synthesized from FA by alkali fusion and hydrothermal treatment. Copper oxide was then immobilized in zeolite framework (CuO/Zeo-NaX) by ion exchange with Cu(II) ion and subsequent calcination process. The catalysts were characterized by X-ray diffraction (XRD), high resolution scanning electron microscope (HRSEM), energy dispersive X-ray (EDX) and diffuse reflectance spectroscopy (DRS) methods. XRD and HRSEM techniques revealed CuO surface nano fringes over zeolite particles. In the visible light degradation of methylene blue (MB) as a model dye, under the optimal experimental conditions of catalyst amount = 0.5 gL^{-1}, [MB] = 20 ppm, pH = 6.8, and temperature = 25°C, the degradation of MB was 80.2%, 59% and 41% with CuO/Zeo-NaX, CuO and Zeo-NaX catalysts respectively. The notable feature of the present catalysts is that the degradation of MB occurred even without H_2O_2. Obviously, the catalyst itself produced the necessary reactive oxygen species which destructed MB. Further, efficiency of the catalyst did not decrease much even after three/four reaction cycles. Altogether, the CuO/Zeo-NaX photocatalyst developed in the present work performed well and is efficient in many respects.

KEYWORDS: Fly ash; zeolite NaX; CuO; Visible light photodegradation; Methylene blue dye.

INTRODUCTION

Development of new, efficient and green methods for the degradation of pollutants in wastewater is an active area of research. The advanced oxidation process (AOP) based on the generation of hydroxyl radical (OH·) is a powerful tool for destructing stable aqueous organic contaminants [1]. Heterogeneous photocatalysis under visible light, one of the advanced oxidation processes, is a widely-applied technique for environmental remediation, especially for wastewater decontamination, due to its high efficiency, renewability, cheap and eco-friendly features [2,3]. Different types of materials are being studied for this process, which include zeolite based photocatalysts [4-6], mixed metal oxides [7], clay supported catalysts [8] etc. In the past few years, various types of commercial, synthetic and natural zeolites supported photocatalysts have been investigated [4-6, 9-11]. However, in the present work the focus is on a new resource for zeolite, namely the coal fly ash (FA). FA is a major solid waste from coal-firing power stations and it poses threats to all the three segments of environment – air, water and soil [12]. Hence in an attempt to use it and thereby to mitigate the pollution from FA, in our previous work [12] we developed zeolite photocatalyst with nano gold

loading and studied the photodegradation of phenolics under visible light [12] and also iron oxide/Zeo-NaX [13] and CeO_2/Zeo-NaX [14] photocatalysts and applied them for dye degradation. In the present work immobilization of CuO as nano fringes is performed in zeolite framework so as to make it visible light photoactive.

Among the various semiconductors, CuO is used as an effective, inexpensive and nontoxic semiconductor photocatalyst for the degradation of a wide range of pollutants [9-12]. CuO is a significant p-type semiconductor with band gap energy of 1.2–1.5 eV. This low band gap enables it to be photoactive in the visible region [15].

In the present work we report for the first time the development of visible light active nano CuO incorporated zeolite photocatalyst and its activity assessment through a model dye methylene blue (MB) degradation. The notable feature of the present catalyst is that the photocatalytic degradation of MB occurred even without H_2O_2. That means the developed catalyst performs well by producing reactive oxygen species like $O_2^{\cdot-}$, $^{\cdot}OH$ etc., even without H_2O_2 and causes the oxidative degradation of MB. Such interesting results are presented herein.

EXPERIMENTAL

Materials

The main raw material, coal fly ash sample (FA) was collected from electrostatic precipitators of nearby thermal power plant, Tuticorin, Tamilnadu. Analytical reagent (AR) grade cupric sulphate was purchased from Merck, Mumbai, India and methylene blue dye of pure grade was from Rankem, India. All the procured chemicals were used without further purification as they were of analytical grade. Throughout the experiment double distilled (DD) water was used. Stock solution 1000 mg/L (1000 ppm) of methylene blue was prepared in DD water, and diluted to desired concentration during degradation experiments. pH of the dye solution was adjusted with aqueous HCl and NaOH solutions.

Pretreatment of FA

The raw fly ash samples were first screened through BSS Tyler siever of 75 mesh size to eliminate larger particles. First the FA was washed with DD water several times. Then the water washed FA was treated with 0.1 M HCl. This acid treatment decreased the concentration of Fe and other oxides (alkali oxides) which were mainly situated on the exterior part of fly ash particles. Also this acid treatment served to increase the activity, thermal stability and acidity of the zeolite, all aiming to better catalytic activity. This pre-treated sample is labeled as PFA.

Synthesis of Zeolite NaX (Zeo-NaX)

Zeolite NaX was synthesized from pretreated FA by alkaline fusion followed by hydrothermal treatment [16,17]. A typical procedure was as follows. The pretreated FA was mixed with sodium hydroxide at 1:1.3 ratio (wt/wt) and fused at 550°C for 1 h. Thereafter, the fused product was mixed with DD water, and the resulting slurry was aged for 20 h and finally crystallized at 90°C for 6 h. After synthesis, the obtained solid product was recovered by filtration and washed with DD water until the pH of the samples was about 9. The product was then dried in a vacuum oven at 60°C for 2 h. The sample was labeled as Zeo-NaX.

Synthesis of CuO/Zeo-NaX

In the preparation of CuO/Zeo-NaX, 3 g Zeo-NaX was suspended in 100 ml of 0.05 M – 1.0 M (different initial concentrations) cupric sulphate solution. The reaction mixture was magnetically stirred for 20 h. Cu(II) exchanged zeolite (Cu/Zeo-NaX) was separated by filtration and washed several times with DD water till the filtrate was free from Cu(II) metal ions. Then it was dried for 12 h at 100$\pm$5°C in an air oven and calcinated in a pre-heated muffle furnace at 450°C for 4 h. The cooled sample was collected, ground and stored in air-tight container.

Synthesis of CuO

Cupric sulphate taken in a silica crucible was heat-treated in a muffle furnace at 950°C for 4 h. Then it was cooled to room temperature and the collected mass was ground, and stored in air-tight container.

Instrumental characterization

Powder X-ray diffraction (XRD) patterns were recorded for the angle 2θ = 10 - 80° in a step of 0.05° in a continuous scanning mode using the instrument, PANalytical Expert Pro-MPD with CuK_a radiation (λ = 1.5406Å) from a generator

set at 30 mA and 40 KV. Diffuse reflectance spectra (DRS) of the catalysts (λ = 200 – 800 nm) were obtained using a Shimadzu 2700 UV-vis spectrophotometer with $BaSO_4$ white background. High Resolution Scanning Electron Microscope (HRSEM) images of the samples were obtained with FEI QUANTA FEG 200 microscope. The integrated energy dispersive X-ray (EDX) spectroscopy was applied to identify and quantify the dispersion of copper in CuO/Zeo-NaX sample using BRUKER instrument. UV-visible spectra of the MB dye solution were obtained in the wavelength range 200-800 nm on Perkin-Elmer spectrophotometer, Lambda 25 model. The oxidized products of MB were analyzed by Alliance 2795 HPLC coupled with a Waters Micromass Quatro triple quadrupole mass spectrometer equipped with electrospray ionization (ESI) and atmospheric pressure chemical ionization (APCI) sources having mass range of 4000 amu in quadrupole and 20000 amu in TOF.

Photocatalytic degradation of MB

The photocatalytic activity of the synthesized catalysts was evaluated from the degradation of MB at the following variable experimental conditions but without using H_2O_2 for hydroxyl radicals generation. The degradation reaction was conducted in an immersion type (Haber photoreactor, model HIPR LC-150) photoreactor fitted with 150 W tungsten halogen lamp (λ ≥ 400 nm; intensity = 14.79 mW/cm² at 550 nm measured with Kusem-Meco Luxmeter, model KM Lux 200k and converted into Watt). The temperature of the reactor solution was maintained constant at 25°C throughout the experiment by using water circulation. pH of the dye solution was adjusted to 6 to 12 by adding 0.1 M NaOH or HCl solution. The suspension was magnetically stirred for about 30 min to establish the adsorption/desorption equilibrium between dye and catalyst. After 30 min, light irradiation was commenced and magnetic stirring was continued. For taking dye sample for spectral recording, lamp was switched off, stirring was stopped and the solution was allowed to stand for 5 min. At given time intervals (20 min), 2 ml dye sample was collected, immediately centrifuged to remove the catalyst and used for subsequent analysis. The degradation was monitored by UV-Visible spectroscopy at 665 nm, the λ_{max} of MB. The degradation percentage was calculated using eqn. (1)

$$\% \text{ degradation} = \frac{[MB]_o - [MB]_t}{[MB]_o} \times 100 \quad \text{----- (1)}$$

Where $[MB]_o$ is the initial concentration and $[MB]_t$ is the concentration at selected time intervals. Since concentration is directly proportional to absorbance according to Beer–Lambert's law, the dye degradation was monitored by absorbance measurements.

The catalytic degradation of MB was investigated for the influence of experimental variables like CuO loading on Zeo-NaX, catalyst dose, initial concentration of MB and pH. For the recycle runs of catalyst, the used catalyst was collected by centrifugation, washed with water, dried at 100°C and used for MB degradation.

RESULTS AND DISCUSSION

Catalysts characterization

The X-ray diffraction (XRD) patterns of pre-treated FA, Zeo-NaX, CuO/Zeo-NaX and also bulk CuO (the inset of Fig. 1) are shown in Fig. 1. The characteristic high intense peaks at 2θ = 26.6° and 2θ = 40.9° together with other major peaks (Fig. 1a) are indicative of the presence of Quartz (Q) and Mullite (M) in PFA. The diffraction pattern of PFA is in good agreement with JCPDS file No. 001-0649. The characteristic lines located at 2θ values of 10.1, 11.8, 15.5, 18.4, 20.09, 23.3, 31.1° etc as observed from XRD pattern b in Fig. 1 can be indexed to Zeo-NaX crystalline planes by matching with the zeolite patterns in the library of XRD patterns [JCPDS No. 39-0218] and also by matching with reports in literature [16,17]. Fig. 1c shows CuO peaks at 2θ = 28.0, 35.5, 38.7 and 48.7° matchable with those of monoclinic CuO (JCPDS No. 05-0661). It is inferable that the Cu exchanged in zeolite framework is converted to CuO during calcination [18]. In the XRD pattern of pristine CuO (inset Fig. 1) characteristic sharp signals are observed at 2θ values of 32.5, 35.5, 38.7, 48.7, 53.4 and 58.3° (JCPDS No. 05-0661) and they indicate monoclinic crystalline phase [18-22]. But the same CuO on Zeo-NaX yields broad signals. These apparently broader peaks for CuO and sharp peaks for crystalline zeolite in Fig. 1c demonstrate unequivocally the

loading of CuO in nano amorphous form over crystalline zeolite network. Further, a comparison of intensity of the sharp signals for pure Zeo-NaX (Fig. 1b) and for CuO/Zeo-NaX (Fig. 1c) reveals that the latter sample has very much reduced value. Evidently it means a decline in crystallinity of Zeo-NaX on CuO incorporation. The % of crystallinity data computed from the two patterns validate this statement. The crystallinity of Zeo-NaX and CuO/Zeo-NaX material are 90.6% and 49.5% respectively. Similar observation on CuO/Zeo-NaX has been made by Nezamizadeh-Ejhieh et al [19] for the synthesis of CuO incorporated nano zeolite X. The same group [11] has also reported that by incorporation of CuO into the nano zeolite X, the peaks intensity significantly decreased with respect to those of the nano zeolite (NX). Another study by Hao et al [21] also showed that by incorporation of CuO into the MCM-41, the peaks intensity decreased with respect to parent MCM-41. CuO species in crystalline form could not be formed on Zeo-NaX, perhaps, due to the dispersion of nano CuO on Zeo-NaX at the maximum surface level (SEM images confirm; discussion follows). Thus more active sites of CuO are produced on zeolite [9-11]. The average crystallite sizes (D) (Scherrer method) of the materials are PFA = 64.73 nm, Zeo-NaX = 51.84 nm and CuO/Zeo-NaX = 57.13 nm. Hence it is concluded that CuO is present in amorphous form in CuO/Zeo-NaX material due to the high dispersion of nano size CuO. A similar observation was reported on the CuO/nanozeoliteX catalyst [18].

The HRSEM images of Zeo-NaX and CuO/Zeo-NaX samples are shown in Fig. 2. SEM image of Zeo-NaX powder consists of predominantly spherical, smooth particles/grains of 1-2 μm in diameter [15]. However, the image of CuO/Zeo-NaX (Fig. 2b) shows irregularly shaped somewhat bigger spongy like particles. A close examination of the image reveals the existence of nano fringes (small densely arranged fibre like structure) on the entire surface of Zeo-NaX particles. The whole morphology of CuO/Zeo-NaX looks like the white spongy fully opened cotton fruit in the plankton. Thus CuO is dispersed in nano fringe form on Zeo-NaX in consistent with the XRD observation [18].

The elemental analysis data of SEM EDX given in (Table. 1) clearly suggest the chemical composition of the materials. The low Si/Al ratio of zeolite (1.12) confirms the formation of Zeo-NaX type. The presence of 22 atomic % of Cu confirms the formation of CuO/Zeo-NaX material.

Table 1: Elemental composition of the materials from SEM-EDX analysis

Material	Element (atomic %)				
	Si	Al	O	Cu	Si/Al
FA	19.24	14.65	55.40	0.01	1.31
Zeo NaX	16.06	14.92	55.86	0.01	1.08
CuO/Zeo NaX	16.33	18.15	5.46	22.39	0.88

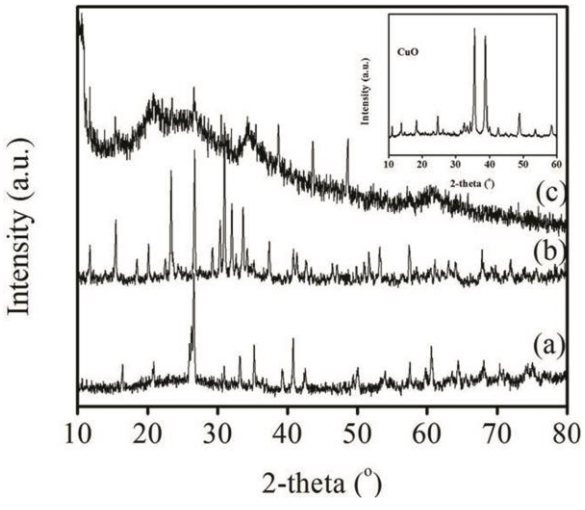

Fig. 1: XRD patterns of (a) PFA, (b) Zeo NaX and (c) CuO/Zeo NaX (inset: CuO)

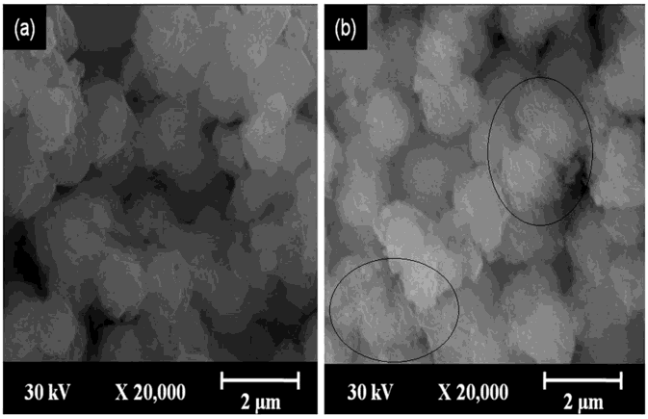

Fig. 2: HRSEM images of (a) Zeo NaX (2 µm) (b) CuO/Zeo NaX (2 µm)

The UV–Vis DRS of Zeo-NaX, CuO and CuO/Zeo-NaX are shown in Fig. 3.1. The spectrum of Zeo-NaX has absorption only upto 500 nm and does not display any characteristic absorption peak in the UV or visible regions [18]. The pure CuO shows a very strong absorption almost in the entire UV and vis region (E_g = 1.2–1.5 eV) with a broad band at 260 nm and another band in the range of 380-500 nm [24] and extends its absorption upto 800 nm. In the case of CuO/Zeo-NaX sample strong absorption commencing from UV extends only upto 320 nm and beyond which it gradually subdues until a minimum is reached at about 550 nm. This absorption upto 550 nm reflects the absorption trend of pristine zeolite Fig. 3i (a). However, for CuO/Zeo-NaX sample the absorption begins to rise after 550 nm, continues to increase and extends upto 800 nm in the visible region [4]. Certainly this absorption, as justified by Fig. 3i (b), is contributed by CuO. Therefore, CuO/Zeo-NaX resembles Zeo-NaX in its first part of absorption spectrum but the latter part is facilitated by CuO. All these DRS results confirm CuO incorporation in Zeo-NaX. Visible light sensitization of zeolite by CuO is thus possible to the entire range of wavelength and CuO/Zeo-NaX could thus be an active visible light photocatalyst [19-22]. E_g values, to be discussed next, also corroborate this finding.

Fig. 3.2 shows $(\alpha h\nu)^2$ versus hν Tauc plots involving direct allowed transition. The values of the band gap E_g are 2.49 eV for CuO/Zeo-NaX, 1.78 eV for CuO and 3.4 eV for Zeo-NaX. These values are in agreement with those reported in literature [19,24].

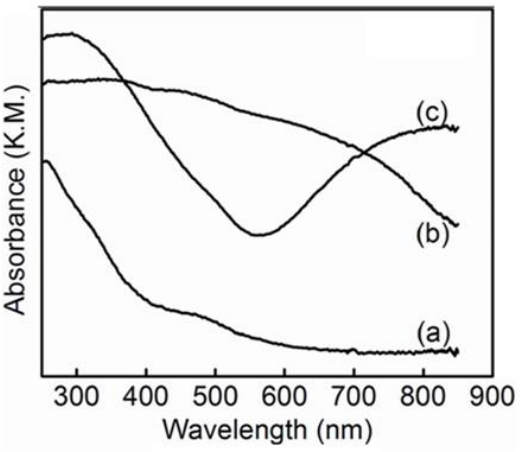

Fig. 3.1

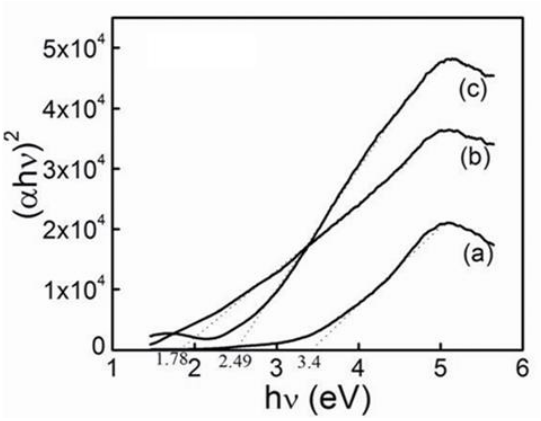

Fig. 3.2

Fig. 3: (1) DRS of (a) Zeo NaX (b) CuO and (c) CuO/Zeo NaX; (2) Tauc plot for (a) Zeo NaX (b) CuO and (c) CuO/Zeo NaX

Evaluation of photocatalytic activity of CuO/Zeo-NaX

Fig. 4a shows the adsorption of MB dye under dark condition over Zeo-NaX, CuO and CuO/Zeo-NaX catalysts. The amounts of adsorption of the photocatalysts are 6.2% for CuO/Zeo-NaX, 41.4% for Zeo-NaX and 0.5% for CuO after 180 min

contact time. The results reveal that Zeo-NaX has greater adsorption for MB dye compared to CuO or CuO/Zeo-NaX. Pristine CuO is a very poor adsorbent for MB. This feature considerably reduces the adsorption tendency of Zeo-NaX on CuO immobilization and consequently CuO/Zeo-NaX, the newly developed catalyst, has only a meager adsorption for MB. CuO, thus, makes Zeo-NaX a better photocatalyst with minimal adsorption capacity.

Fig. 4b shows a comparison of photodegradation of MB dye under visible light over Zeo-NaX, CuO and CuO/Zeo-NaX catalysts in the absence of H_2O_2. Zeo-NaX and CuO individually exhibit 41.4% and 59% of degradation of MB upto 180 min time duration. In contrast, CuO/Zeo-NaX exhibits 80.2% degradation efficiency under the same condition. This result clearly shows that the presence of CuO in Zeo-NaX greatly enhances the degradation efficiency and renders CuO/Zeo-NaX an optimized photocatalyst. The obtained result is not only in consistent with the results of XRD, SEM and EDX but also validates the supposition arrived at from these characterizations that CuO/Zeo-NaX could be a better photocatalyst. Similar observations on the salient feature of CuO in zeolite have been reported in previous works [9-11,19,22,23].

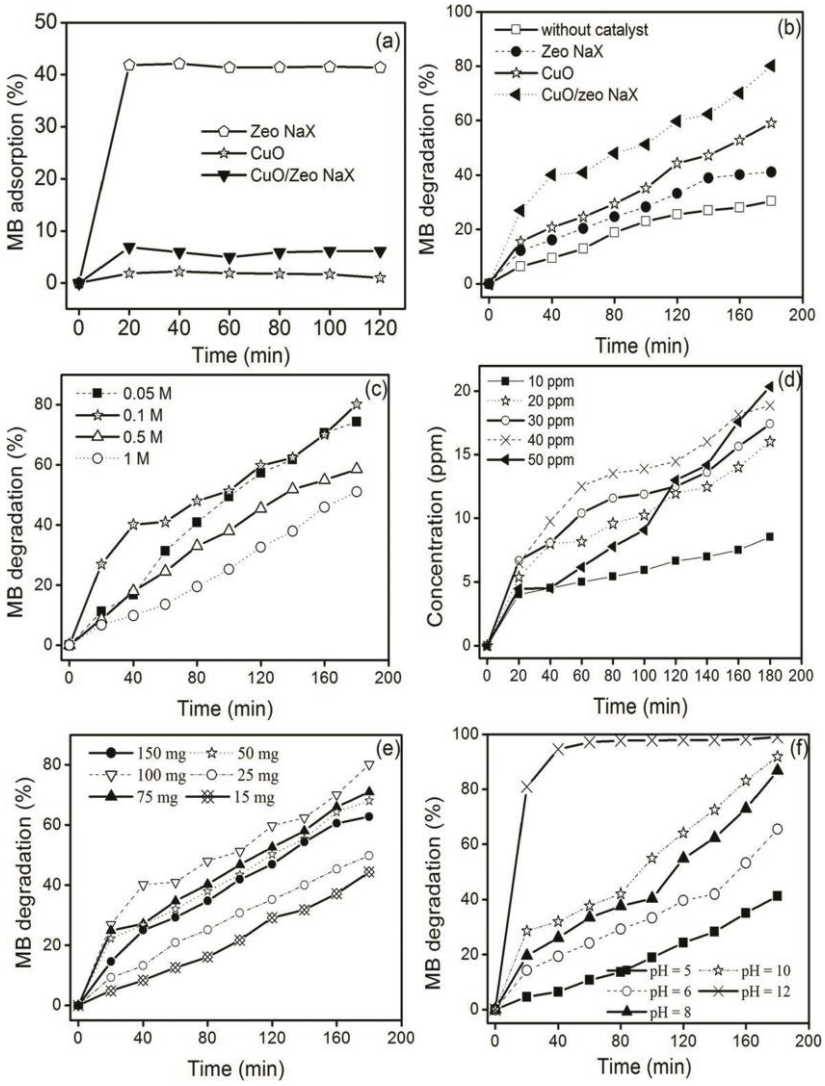

Fig. 4: Effect of experimental variables on MB degradation by CuO/Zeo NaX without H_2O_2; (a) Effect of various catalysts on MB adsorption in dark (500 mg/L catalyst, 20 ppm dye, pH = 6.8); (b) Effect of various catalysts on MB photodegradation (500 mg/L catalyst, 20 ppm dye, pH = 6.8); (c) Effect of CuO loading at different levels (500 mg/L catalyst, 20 ppm dye, pH = 6.8); (d) Effect of initial dye concentration (catalyst dosage 500 mg/L, pH = 6.8) (e) Effect of catalyst dosage (20 ppm dye, pH = 6.8); (f) Effect of pH (catalyst dosage 500 mg/L, 20 ppm dye)

CuO/Zeo-NaX being arrived at as the optimal catalyst, the next essential part of the investigation is the study of influence of various experimental parameters on photodegradation. A systematic variation of CuO loading, catalyst dose, initial concentration of dye and pH has been performed and the results are discussed in following sections.

Effect of CuO loading

CuO loading on Zeo-NaX was done with different initial concentrations (0.05 – 1.0 M) of cupric sulphate and four different CuO/Zeo-NaX catalysts were prepared and applied for MB degradation (Fig. 4c). % of dye degradation increases with the increase in CuO loading upto 0.1 M Cu^{2+} solution and thereafter it decreases which is possibly due to the existence of aggregated CuO sites on Zeo-NaX and the consequent shielding of core/inner zeolite particle and its activity prohibition (CuO alone tends to exhibit the activity). Another possible reason is the shielding of incident light [3,26]. 0.1 M $CuSO_4$ solution is found to yield the optimal CuO loading. A similar observation was reported on the photocatalytic degradation of mixture of MB and MO using CuO/nanozeoliteX catalyst [11,20,21].

Effect of dye concentration

The effect of initial dye concentration (10-50 ppm) on degradation of MB was studied and the result is shown in Fig. 4d. From 10-40 ppm concentration, the amount of dye degraded increases, at 40 ppm it reaches maximum and beyond this, it declines. 40 ppm is the optimal dye concentration where the maximum dye degradation is observed. Perhaps, at this dye concentration, there is sufficient amount of hydroxyl radicals which destruct the dye.

If % of degradation instead of concentration (Fig. 4d) is considered, the trend observed is quite different. The % of degradation for 10, 20, 30, 40 and 50 ppm dye concentration are 85, 80.2, 58.1, 47.7 and 40.7 respectively for 180 min reaction time at pH 6.8 and with a catalyst dose of 500 mg/L^{-1}. 10 and 20 ppm are close and hence they appear to be optimal dye concentrations. Further experiments were, therefore, done with 20 ppm dye. The decrease in amount of dye degraded beyond 40 ppm is attributable to the fact that the dye will start acting as a filter for the incident light, thus reducing light penetration [3,26] and light reaching the photocatalyst [19].

Effect of dosage of the catalyst

The result of effect of catalyst dosage on degradation of MB is shown in Fig. 4e. Photocatalytic degradation of MB was studied at catalyst dosages of 75, 125, 250, 500, 750 mg/L under optimal conditions of 20 ppm dye and pH 6.8. The depicted results in Fig. 4e reveal that with an increase in dose of catalyst from 75 mg/L to 500 mg/L the per cent of degradation increases and thereafter decreases. Increase in % of dye degradation with catalyst dose is caused by an increase in number active sites available for dye degradation under optimal penetration of radiation through suspension [3]. Above 500 mg/L, the % decrease of MB occurs, possibly due to the increase in opacity of the solution with the excessive amount of catalyst in the reaction, leading to attenuation [19,25]. Therefore, an optimum catalyst dose is 500 mg/L.

Effect of pH

Industrial wastewater usually has a wide range of pH values. Generally pH influences the photocatalytic degradation of organic pollutants. In this study the effect of pH was examined by fixing the initial pH of the reaction mixture at 5, 6, 8, 10 and 12 under optimal conditions of 20 ppm dye and 500 mg/L catalyst. As it is seen from Fig. 4f, the per cent of photocatalytic degradation of MB, increases with increase in pH and the maximum degradation efficiency is obtained at alkaline pH of 12 (100%). When the pH of the solution is raised from 10 to 12, there is an abrupt increase in % of degradation from the beginning itself in the 0-180 min duration. The degradation reaction is faster and dye degradation is 100% complete within 100 min time. This trend is explicable by the well-known fact as the pH of the solution is in the alkaline side, more hydroxide ions are available, which will generate more hydroxyl radicals by combining with the catalyst and these extra hydroxyl radicals are responsible for the observed enhancement in photocatalytic degradation of MB [20,27].

Possible mechanism of photoactivation and photodegradation of MB

A schematic of the mechanism of MB dye degradation is displayed in Fig. 5A. CuO functions as visible light sensitizer. On band gap excitation with light, e^- - h^+ pair is formed. Zeo-NaX traps e^- and the trapped e^- reacts with oxygen present in air being bubbled through reactor solution and produces superoxide radical which on reaction with water produces hydroxyl radical. The h^+ present in VB of CuO also reacts with water and produces hydroxyl radical and in this process CuO is regenerated. The $^{\cdot}OH$ and $O_2^{\cdot-}$ are the probable reactive oxygen species which oxidatively degrade MB and mineralize it [28,29]. A sequence of reactions/processes given in eqns. 2 – 13 illustrates the dye degradation mechanism.

$$CuO \xrightarrow{h\nu} e^-_{CB} + h^+_{VB} \quad (2)$$

$$(H_2O \longleftrightarrow H^+ + OH^-) + h^+_{VB} \longrightarrow H^+ + {}^{\bullet}OH \quad (3)$$

$$O_2 + e^-_{CB} \longrightarrow O_2^{\bullet-} \quad (4)$$

$$O_2^{\bullet-} + H^+ \longrightarrow HO_2^{\bullet} \quad (4a)$$

$$HO_2^{\bullet} \longrightarrow H_2O_2 + O_2 \quad (4b)$$

$$CuO\,(Cu^{2+}) + e^-_{CB} \longrightarrow CuO\,(Cu^{+}) \quad (5)$$

$$CuO\,(Cu^{+}) + O_2 \longrightarrow CuO\,(Cu^{2+}) + O_2^{\bullet-} \quad (6)$$

$$H^+ + O_2^{\bullet-} \longrightarrow HO_2^{\bullet} \quad (7)$$

$$CuO\,(Cu^{+}) + HO_2^{\bullet} + H^+ \longrightarrow CuO\,(Cu^{2+}) + H_2O_2 \quad (8)$$

$$H_2O_2 + e^-_{CB} \longrightarrow OH^- + {}^{\bullet}OH \quad (9)$$

$$H_2O_2 + h^+_{VB} \longrightarrow {}^{\bullet}OH + H^+ \quad (10)$$

$$Dye \xrightarrow{h\nu} Dye^{\bullet} \quad (11)$$

$$Dye^{\bullet} + {}^{\bullet}OH \longrightarrow \text{Degradation of dye} \quad (11a)$$

$$Dye + h^+_{VB} \longrightarrow \text{Oxidation of dye} \quad (12)$$

$$Dye + e^-_{CB} \longrightarrow \text{Reduction of dye} \quad (13)$$

Reusability of the photocatalyst

The stability and reusability of catalysts are very important issues for practical applications. Fig. 5B shows the graphical picture of reusability of CuO/Zeo-NaX for MB photodegradation. Each experiment was done under the optimal condition of 20 ppm dye, 500 mg/L catalyst dose and pH of 6.8. As seen from Fig. 5B, there is no apparent loss of degradation efficiency from the first cycle to the third cycle. But during fourth cycle, degradation efficiency is marginally decreased. This might have been caused by incomplete removal of byproducts of MB. Also a general reason for the decrease in catalytic activity is the affixing of reaction intermediates on the catalyst surface, which thus deactivate the corresponding active sites.

Physico-chemical stability of the catalyst

The physico-chemical stability of the spent/used catalyst was examined through FTIR and DRS characterizations. FTIR spectrum of used catalyst (Fig. 5C) has similarity to the spectrum of fresh CuO/Zeo-NaX. Also in the FTIR spectrum of used catalyst no characteristic peaks from MB dye could be found. Fig. 5D shows the similar DRS of fresh and used catalysts. Thus FTIR and DRS study shows that the used catalyst material has chemical structure/groups equivalent to fresh catalyst, and hence it is concludable that the chemical stability of the catalyst is maintained during three/four reaction cycles.

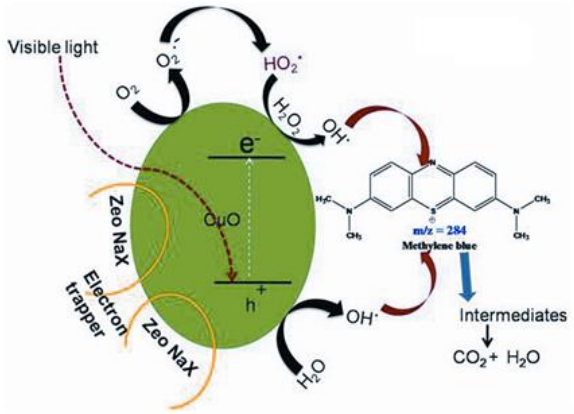

Fig. 5A

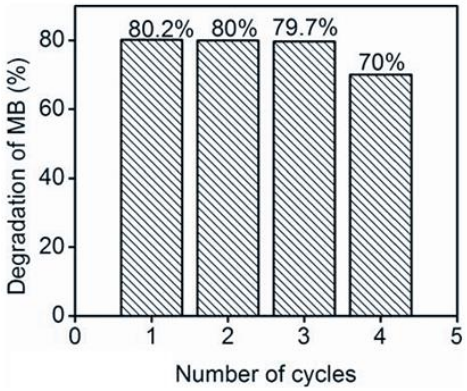

Fig. 5B

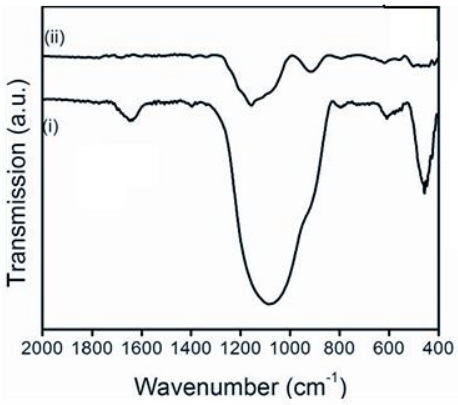

Fig. 5C

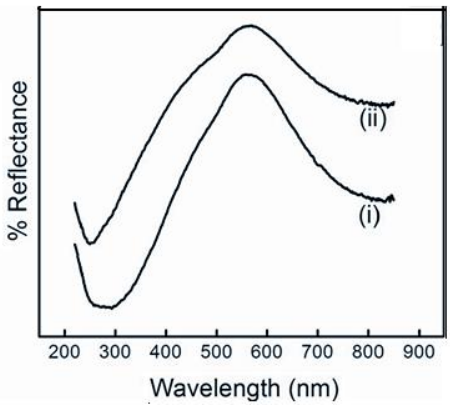

Fig. 5D

Fig. 5 : (A) Possible mechanism of photoactivation of catalyst and degradation of MB with CuO/Zeo NaX; (B) Reusuability study of CuO/Zeo NaX; (C) FTIR spectra of CuO/Zeo NaX catalyst (i) before and (ii) after MB degradation; (D) DRS of CuO/Zeo NaX catalyst (i) before and (ii) after MB degradation

Comparison of degradation efficiencies of present and previous catalysts

Solar photodecolorisation of MB by CuO/X zeolite was reported as 86.8% (at 0.01 mM dye i.e., 2.84 ppm) after 180 min of irradiation time [20]. The photocatalytic activity of titania modified mesoporous silica was roughly 90% for MB solution of 10 mg/L after 180 min of irradiation time [30]. CuO in the presence of oxidizing agent H_2O_2 showed 97% degradation of MB (conditions: 10 mg/L dye, 20 ml H_2O_2 and 20 mg catalyst) after 10 h irradiation [31]. Batista et al. [32] reported MB dye degradation by CuO/SiO_2 under UV irradiation in the presence of H_2O_2 and achieved 100% degradation of 100 mg/L dye using 1 ml H_2O_2 (30 wt%) 30 mg of catalyst in 120 min of irradiation time. Considering the fact of the present work that MB degradation was performed at higher dye concentration under visible light irradiation for 3 h in the absence of oxidizing agent H_2O_2, the results clearly indicate the superiority of the present catalyst over the past ones. Compared with the above-cited and other previous reports in literature [7,9-11,13-16,24] the present work highlights the potentiality of CuO/Zeo-NaX catalyst. Further, the highlighting point of the present work is that many of the previous studies use zeolite X synthesized from silica and alumina precursors (chemical precursor) [11,19], but herein zeolite NaX was synthesized from cheap and easily available waste material coal fly ash. Thus a solid waste pollutant is converted in to a usable catalyst product.

LC-MS with ESI-Mass studies for product analysis

MB photodegradation reaction was investigated by HPLC-(-ESI)-TOF-MS for the identification of intermediates. Fig. 6 shows the mass spectra of MB after degradation for 180 min. The fresh MB gives a high intense single peak at m/z = 284

corresponding to the M^+ molecular ion of MB [32]. However, in the present case, after 180 min reaction the parent peak of MB is seen only with a decreased intensity in Fig. 6 along with various new peaks, indicating that the dye is broken down and new products are formed.

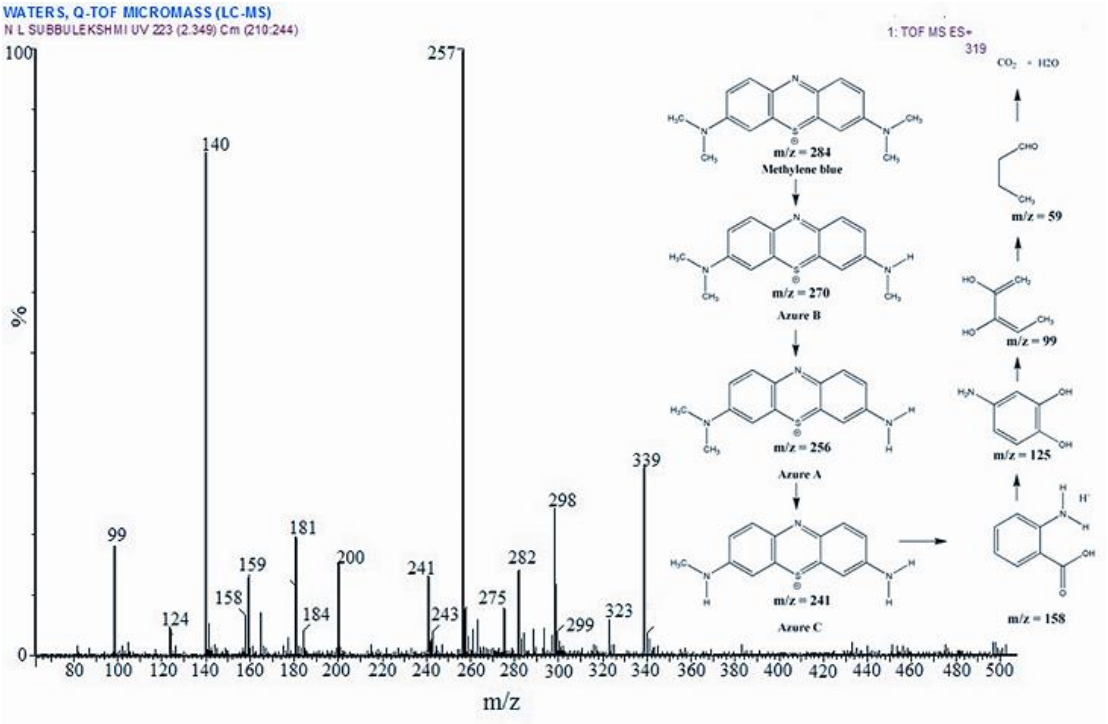

Fig. 6: HPLC-ESI-MS spectra of products from MB photodegradation for 180 min, 20 ppm MB and pH = 6.8. The inset chemical structures display the possible photodegradation pathway.

The analysis of mass spectrum in Fig. 6 suggests a sequence of degradation mechanism (given as inset in Fig. 6), in which the hydroxyl radical preferentially attacks the chromophore center of the dye molecule, with the bond cleavage and release of one or more of the methyl group substituents on the amine groups, leading to formation of azure A, B and C and thionin [33,34]. Finally opening of aromatic rings takes place and the resultant smaller intermediates undergo several degradation reactions to yield CO_2. Thus LCMS data, thus, confirm photocatalytic degradation and mineralization of MB dye. Since the whole reaction was performed without H_2O_2, the LCMS data also provide evidence to the fact that MB has undergone degradation by $^{\bullet}OH$ and other reactive species produced by the catalyst.

CONCLUSION

In the present work a new visible light active zeolite photocatalyst has been successfully developed from the waste material coal fly ash by alkali fusion and hydrothermal techniques and subsequent CuO immobilization. All the instrumental characterizations confirm the formation of Zeo-NaX and CuO/Zeo-NaX catalysts. XRD and HRSEM techniques show the presence of CuO in amorphous nano surface fringes over zeolite. The DRS study clearly shows that CuO extends the visible light absorption of zeolite upto 800 nm and reduces its E_g value from 3.4 to 2.49 eV. The visible light degradation of MB dye was catalysed by Zeo-NaX, CuO and CuO/Zeo-NaX even without H_2O_2 (normally applied oxidant) and the activities are in the above increasing order. CuO incorporation thus improves the visible light response of zeolite and enhances remarkably its catalytic activity. The developed catalyst CuO/Zeo-NaX is thus more efficient, chemically stable and is found rugged for several catalytic runs. Besides these features, the new catalyst being derived from waste coal fly ash is cost effective to commercial zeolite. Altogether, a new, efficient

and cost effective zeolite photocatalyst has emerged which can function even without H_2O_2.

CONFLICT OF INTEREST

The authors declare that there is no conflict of interest

REFERENCES

1. Hoffmann MR, Martin ST, Choi WY, Bahnemann DW. Environmental applications of semiconductor photocatalysis. Chem Rev. 1995; 95: 69-96.
2. Mills A, Hunte L. An overview of semiconductor photocatalysis. J Photochem Photobiol A: Chem 1997; 108: 1-35.
3. Akpan UG, Hameed BH. Parameters affecting the photocatalytic degradation of dyes using TiO_2-based photocatalysts: A review. J Hazard Mat 2009; 170: 520-529.
4. Najafabadi AT, Taghipour F. Cobalt precursor role in the photocatalytic activity of the zeolite-supported TiO_2-based photocatalyst under visible light: A promising tool toward zeolite based core-shell photocatalysis. J Photochem Photobiol A: Chem 2012; 248: 1-7.
5. Guo Y, Zu B, Dou X. Zeolite-based photocatalysts: A promising strategy for efficient photocatalysis. J Thermodyn Catal 2013; 4: e120.
6. Corma A and Garcia H. Zeolite-based photocatalysts. Chem Commun 2004; 1443-1459.
7. Hui-Li X, Hui-Sheng Z, Tao Z, Dong-chang X. Photocatalytic degradation of acid blue 62 over CuO-SnO_2 nanocomposite photocatalyst under simulated sunlight. J Environ Sci 2007; 19: 1141-1145.
8. Sohrabnezhad SH, Mehdipour Moghaddam MJ, Salavatiyan T. Synthesis and characterization of CuO-Montmorillonite nanocomposite by thermal decomposition method and antibacterial activity of nanocomposites. Spectrochim Acta A 2014; 125: 73-78.
9. Nezamzadeh-Ejhieh A, Amiri M, CuO supported clinoptilolite towards solar photocatalytic degradation of p-aminophenol. Powder Technol 2013; 235: 279-288.
10. Nezamzadeh-Ejhieh A, Salimi Z, Heterogeneous photodegradation catalysis of o-phenylenediamine using CuO/Xzeolite. Appl Catal A: Gen 2010; 390: 110-118.
11. Nezamzadeh-Ejhieh A, Shamsabadi MK. Decolorization of binary azo dyes mixture using CuO incorporated nanozeolite-X as a heterogeneous catalyst under solar irradiation. Chem Eng J 2013; 228: 631-641.
12. Anusha JV, Bala Nambi A, Subramanian E. In Situ and Ex Situ Immobilization of Nano Gold Particles in Zeolite Framework and a Comparison of Their Photocatalytic Activities. J Inorg Organomet Polym Mater 2018; 28:15–26.
13. Sudha G, Subramanian E, Murugan C. Development of iron oxide/zeo NaX nano photocatalyst from coal fly ash and its activity assessment by methylene blue degradation. Int Res J Nat Appl Sci 2015; 2(2): 114-128.
14. Sudha G, Subramanian E. Synthesis, characterization and photocatalytic study of Cerium oxide/Zeo-NaX catalyst with brilliant green dye degradation. J Adv Chem Sci 2015; 1(3): 117-120.
15. Saravanan R, Karthikeyan S, Gupta VK, Sekaran G, Narayanan V, Stephan A. Enhanced photocatalytic activity of ZnO/CuO nanocomposite for the degradation of textile dye on visible light illumination. Mater Sci Eng A 2013; 33: 91-98.
16. Amaladhas TP, Thavamani SS, Encapsulation of N, N'-ethlenebis(salicylamide) metal complexes in fly ash based zeolite, characterization and catalytic activity. Adv Mat Lett 2013; 4(9): 688-695.
17. Ojha K, Pradhan NC, Samantha A. Zeolite from fly ash: synthesis and characterization. Bull Mater Sci 2004; 27: 555-564.
18. Treacy MMJ and Higgins JB. Collection of simulated xrd powder patterns for zeolites, Structure commission of the international zeolite association. 4th revised Ed. New York: Elsevier publication; 2001, p148.
19. Nezamzadeh-Ejhieh A, Shamsabadi MK. Comparison of photocatalytic efficiency of supported CuO onto micro and nano particles of zeolite X in photodecolorization methylene blue and methyl orange aqueous miture. Appl Catal A: Gen 2014; 477**:** 83-92.

20. Nezamzadeh-Ejhieh A, Hushmandrad SH. Solar photodecolorization of methylene blue by CuO/X zeolite as a heterogeneous catalyst. Appl Catal A: Gen 2010; 388: 149-159.
21. Hao XY, Zhang YQ, Wang JW, Zhou W, Zhang C, Liu SH. A novel approach to prepare MCM-41 supported CuO catalyst with high metal loading and dispersion. Microporous Mesoporous Mat 2006; 88: 38-47.
22. Ting C, Zhifeng L, Xuerong Z, Zhichao L, Yajun L, Wei L, Bo W. Zeolite-based CuO nanotubes catalyst: investigating the characterization, mechanism, and decolorisation process of methylene blue. J Nanopart Res 2014; 16: 2608-2619.
23. Liou RM, Chen SH. CuO impregnated activated carbon for catalytic wet peroxide oxidation of phenol. J Hazard Mat 2009; 172: 498-506.
24. Jalil AA, Satar MAH, Triwahyono S, Setiabudi HD, Kamarudin NHN, Jaafar NF, Sapawe N, Ahamed R. Tailoring the current density to enhance photocatalytic activity of CuO/HY for decolorization of malachite. J Electroanal Chem 2013; 701: 50-58.
25. Fathima NN, Aravindhan R, Rao JR, Nair BU. Dye house wastewater treatment through advanced oxidation process using Cu-exchanged Y zeolite: A heterogeneous catalytic approach. Chemosphere 2008; 70: 1146-1151.
26. Neren Okte A, Yılmaz O. Characteristics of lanthanum loaded TiO_2-ZSM-5 photocatalysts: Decolorization and degradation processes of methyl orange. Appl Catal A: Gen 2009; 354: 132-142.
27. Huang M, Xu Ch, Wu Z, Huang Y, Lin J, Wu J. Photocatalytic discolorization of methyl orange solution by Pt modified TiO_2 loaded on natural zeolite. Dyes Pigm 2008; 77: 327-334.
28. Paschoalino M, Guedes NC, Jardim W, Mielczarski E, Mielczarski JA, Bowen P, Kiwi J. Inactivation of E.coli mediated by high surface area CuO accelerated by light irradiation >360 nm. J Photochem Photobiol A: Chem 2008; 199: 105-111.
29. Li Y, Lu Y, Zhu X. Photo-Fenton discoloration of the azo dye X-3B over pillared bentonite containing iron. J Hazard Mat B 2006; 132: 196-201.
30. Belhekar AA, Awate SV, Anand R. Photocatalytic activity of titania modified mesoporous silica for pollution control. Catal Commun 2002; 3: 453-458.
31. Yang M, He J. Fine tuning of the morphology of copper oxide nanostructures and their application in ambient degradation of methylene blue. J Colloid Interface Sci 2011; 355: 15-22.
32. Batista A, Carvalho H, Luz G, Martins P. Preparation of CuO/SiO_2 and photocatalytic activity by degradation of methylene blue. Environ Chem Lett 2010; 8: 63-67.
33. Hisaindee S, Meetani MA, Rauf MA. Application of LC-MS to the analysis of advanced oxidation process (AOP) degradation of dye products and reaction mechanisms. Anal Chem 2013; 49: 31-44.
34. Small JM, Hintelmann H. Methylene blue derivatization then LC-MS analysis for measurement of trace levels of sulfide in aquatic samples. Anal Bioanal Chem 2007; 387: 2881-2886.

Cite this article as:
N. L. Subbulekshmi, E. Subramanian. Nano CuO immobilized zeolite photocatalyst from coal fly ash for visible light photodegradation of methylene blue without H_2O_2. J Pharm Chem Biol Sci 2018; 6(2):85-96